AM1, INDO/S and optical studies of carbocations of carotenoid molecules. Acid induced isomerization

Valery V. Konovalov † and Lowell D. Kispert *

Department of Chemistry, BOX 870336, University of Alabama, Tuscaloosa, AL 35487. E-mail: lkispert@bama.ua.edu

Received (in Gainesville, FL) 20th January 1998, Revised 15th January 1999, Accepted 27th January 1999

The mechanism of *trans–cis* isomerization of carotenoid molecules through the formation of the carotenoid carbocation ($CarH^+$) intermediate in the presence of acid is presented. Various *cis*-isomers of carotenoids (β-carotene, canthaxanthin and 8′-apo-caroten-8′-al) are predicted from AM1 calculations of rotation barriers for $CarH^+$, as well as from the stabilities of $CarH^+$. AM1 dipole moments *D* and INDO/S optical transitions of $CarH^+$ were calculated for all protonation sites. Optical spectra of $CarH^+$ solutions exhibit broad lines in the region of 700–1000 nm with extinction coefficients of 1–3 × 10^5 M^{-1} cm^{-1}.

Introduction

Carotenoids (Car) play important functions in nature being light harvesting antenna pigments and photoprotecting agents in photosynthesis.[1–8] Antioxidant properties of β-carotene, a precursor of vitamin A,[9] have been demonstrated, including the quenching of singlet oxygen[10–12] and the trapping of free radicals.[13–17] It is also a potential anticarcinogenic agent.[18–21] Although *in vitro* all-*trans* isomers of isolated carotenoid molecules were found to be the most stable, *in vivo* carotenoids are often present as *cis*-isomers. Thus, 15-*cis* β-carotene was found in the reaction center of spinach photosystem II[5] and photosystem I,[6] and 15-*cis* spheroidene is bound to the reaction center of Rhodobacter sphaeroides.[7] The photoprotective function of carotenoids in photosynthesis is related to isomerization of the excited states of *cis*-isomers into all-*trans* ground states. It has been shown that photoexcited 15-*cis* β-carotene isomerizes into all-*trans via* the T_1 state.[8] The isomerization of 11-*cis* retinal to all-*trans via* the S_1 state is responsible for the primary process of vision.[22] Noticeable thermal *cis*-isomerization of all-*trans* carotenoids at human body temperature (37 °C) indicates that different carotenoid *cis*-isomers may play primary physiological roles.[8,23,24] It has been predicted that di-radical transient states of carotenoids produced by twisting around a polyene chain double bond should be effective radical traps.[23,24] The thermal *cis–trans* isomerization of carotenoids has been extensively studied.[8,23–27] After heating of all-*trans* β-carotene at low temperatures (35–60 °C) for several hours, only 15-*cis* and 13-*cis* isomers were identified.[23] Heating at 190 °C for 15 minutes produced 18 *cis*-isomers.[25,26] A total of 272 *cis*-isomers of polyenes with 9 conjugated double bonds is possible.[23]

Among different methods of geometrical isomerization of all-*trans* carotenoids, little attention has been paid to the mechanism of acid-induced carotenoid isomerization. It has been demonstrated that the presence of small amounts of HCl in dichloromethane solution causes *cis*-isomerization of dissolved carotenoids.[28] The presence of acid in solvents can affect the experimental results on thermo-isomerization of dissolved carotenoids. Adsorption of carotenoids on surfaces in the presence of Brønsted acid sites may result in carbocation formation; a carbocation was observed for the reaction of propene in acidic zeolite-Y.[29]

It is known that acids can catalyze *cis–trans* isomerization of compounds containing double bonds through the formation of an intermediate carbocation. Protonation of a carotenoid molecule at an sp^2 double bond carbon would result in sp^3 hybridization and the formation of a single bond. Subsequently, free rotation about the new single bond would then form *cis*-isomers according to the following mechanism:

$$(Car)_{trans} + H^+ \overset{pK_{BH}}{\rightleftharpoons} (CarH^+)_{trans} \quad (1)$$

$$(CarH^+)_{trans} \rightleftharpoons (CarH^+)_{cis} \quad (2)$$

$$(CarH^+)_{cis} \rightleftharpoons (Car)_{cis} + H^+ \quad (3)$$

The existence of stable carbocations of organic molecules in the presence of strong acids is well known.[30,31] For carotenoids it has been known that an addition of carotenoids to concentrated acids produces deeply colored blue solutions.[32] Wassermann studied proton–acceptor properties of α- and β-carotene mixtures in benzene solutions by addition of trichloroacetic acid or HCl.[33] New near-infrared absorption bands with $\lambda_{max} = 960$ nm and 920 nm, which appeared immediately after the acid addition, were attributed to the formation of ion-pairs ($CarH^+ \cdots A^-$) [equilibrium (4)] and an equilibrium

$$Car + AH \overset{K}{\rightleftharpoons} (CarH^+ \cdots A^-) \quad (4)$$

constant (about 0.4 M^{-1}), *K*, was estimated. The electrical conductivity of the acid–carotenoid solution in benzene lead to the conclusion that the ion-pair ($CarH^+ \cdots A^-$) dissociates to form the charged species[34] with a dissociation constant K_d of about 10^{-8} M [equilibrium (5)]. Later Sorensen obtained solutions of

$$(CarH^+ \cdots A^-) \overset{K_d}{\rightleftharpoons} CarH^+ + A^- \quad (5)$$

a number of relatively stable aliphatic polyenylic cations in concentrated sulfuric and other strong acids, and the structure of the cations was elucidated by ^1H NMR spectroscopy.[30,35] Since

† On leave from the Institute of Chemical Kinetics and Combustion SB RAS, 630090 Novosibirsk, Russia. Present address: NSF Center for Materials for Information Technology, University of Alabama, PO Box 870209, Room 205 Bevill Build. Tuscaloosa, AL 35487. E-mail: vvk01@bama.ua.edu

then few attempts to study carotenoid carbocations were made. For a CH_2Cl_2 solution of all-*trans* carotenoids treated with water, the intermediacy of protonated carotenoids was considered and semi-empirical AM1 calculations of charge densities for a few possible protonation sites were carried out.[28] It was suggested that free rotation about the bond near the carbon atom having the most positive charge gave rise to different geometrical isomers. However, to predict the yield of different *cis*-isomers according to the mechanism (1)–(3), the relative energies of all protonated forms of the carotenoids have to be considered and the barrier for rotation about each polyene chain bond in $CarH^+$ has to be estimated.

The objective of this paper is to extend the previous study of acid induced isomerization of carotenoid carbocations and the roles they play. The AM1 heats of formations, ΔH_0, of $CarH^+$ as well as their dipole moments D and INDO/S optical transitions were calculated for all protonation sites of **1**–**3**. Symmetrical carotenoids **1** and **2** demonstrate the influence of polar substituent (oxygen) on the carbocation properties; **3** was chosen as the most common asymmetrical carotenoid. Possible *cis*-isomers carotenoids due to acid-induced isomerization are predicted. Experimental optical spectra of $CarH^+$ are reported.

Experimental

β-Carotene (**1**) was supplied by Sigma, canthaxanthin (**2**) by Fluka, 8′-apo-caroten-8′-al (**3**) by Hoffmann-La Roche. Purity of the samples was checked by ^{1}H-NMR (360 MHz, $CDCl_3$) and TLC analyses. The carotenoids were stored in the dark at −14 °C in a desiccator containing activated $CaSO_4$ and were allowed to warm to room temperature just before use. Acetonitrile (HPS, Burdick and Jackson), CH_2Cl_2 (anhydrous 99+%, Aldrich), benzene (ASC, Fisher) and trifluoroacetic acid (99%, Aldrich) were used as received. The samples were prepared in a dry box in a nitrogen atmosphere and sealed with parafilm or a rubber septum. Optical absorption spectra were recorded with a Shimadzu UV-1600 spectrophotometer (190–1100 nm). The quartz cuvettes (optical length of 1 cm) were closed with rubber septa stoppers and additional solutions were injected with microsyringes.

AM1 and INDO/S calculations were carried out using HyperChem™ 5.0 software with a P5/233 personal computer. The calculation limit of the energy gradient during the geometry optimization by AM1 was chosen as 0.1–0.2 kcal mol^{-1} Å^{-1}.

Results and discussion

AM1 calculation of carotenoid carbocations

AM1 calculations with full geometry optimization were made for compounds **1**–**3** protonated at all possible positions. The relative heats of formations $\Delta\Delta H_0$ of carbocations $CarH^+$ with respect to the protonated form with the lowest heat of formation, as well as their dipole moments, D, are presented in Table 1. It is seen that calculated stabilities of carbocations are sufficiently different. For compounds **1** and **2,** the lowest ΔH_0 is found for $CarH^+$ obtained by protonation at C7 and for **3** at C9′. According to AM1 calculations, the protonation sites resulting in the lowest ΔH_0 are not those with the highest electron density in the starting molecule. For example, for **2** and **3** the most favored protonation site was found not at oxygen (as was considered before[28]), but at a chain carbon atom. Extensive delocalization energy of the excess positive charge throughout the large number of conjugated double bonds in the polyene chain makes such protonation competitive with protonation of the electronegative oxygen. Formally the largest number of resonance structures of carbocations can be drawn for the terminal protonations, *i.e.* C5, however as a result of poor conjugation of the C5=C6 double bond of the trimethylcyclohexenyl ring with the polyene chain (for the $CarH^+$ of **1** with protonation at C5, the torsion angle of atoms C8–C7–C6–C5 is −20.6°) the enthalpy of those $CarH^+$ is not the lowest.

Table 1 AM1 relative heats of formation of carbocations ($\Delta\Delta H_0$/kcal mol^{-1}) and their dipole moments (D/Debyes)

Protonation position	**1**		**2**		**3**	
	$\Delta\Delta H_0$	D	$\Delta\Delta H_0$	D	$\Delta\Delta H_0$	D
Oxygen	—	—	3.4	32.06	0.54	14.32
C5	3.63	8.94	1.55	4.33	6.02	5.092
C6	33.2	48.72	48.22	49.95	31.93	35.88
C7	0	11.46	0	5.53	3.6	5.30
C8	23.47	46.54	30.74	45.89	19.2	34.36
C9	4.12	15.88	3.28	10.56	9.32	12.48
C10	13.65	40.92	18.72	38.76	12.64	29.08
C11	1.29	19.26	1.64	14.83	8.26	17.35
C12	12.8	38.17	13.33	34.87	8.26	17.35
C13	5.73	23.4	5.48	19.3	14.85	23.02
C14	5.56	30.98	6.3	27.46	5.03	19.34
C15	5.41	27.51	4.84	23.93	15.62	27.92
C15′	—		—		2.86	16.34
C14′	—		—		19.12	33.44
C13′	—		—		4.12	12.88
C12′	—		—		35.3	37.9
C11′	—		—		0.56	9.05
C10′	—		—		48.26	39.52
C9′	—		—		0	6.26

AM1 calculated bond lengths and charges on polyene chain carbons for carbocations with the lowest heats of formation are shown in Figs. 1–3. It is apparent that the excess positive charge is delocalized over the chain to an extent depending on the protonation position. The protonation affects the C–C bond lengths in the chain, but not those in the trimethylcyclohexenyl ring or those between the chain and methyl carbons. The structures of the most stable carbocations are shown in Figs. 4–6. Single bonds were drawn for bond lengths l > 1.4175 Å, dashed bonds (1.5 bond order) for 1.4175 Å ≥ l ≥ 1.3725 Å and double bond for l < 1.3725 Å (note that for the polyene chain of **1**–**3,** the length of the double bond is about 1.35 Å and the single bond is about 1.44 Å). The regular alternating order of single–double bonds changes in $CarH^+$ for all cases of protonation at the chain (compounds **1**–**3**), and remains the same as in the starting all-*trans* compound for protonation at oxygen (**2**, **3**). For all carotenoids, a cluster of approximately 1.5 bond order is observed with the position depending on the protonation site. Note that the charge and bond length distribution is different for carbocations of **1** and **2** protonated at the same position, *i.e.* the terminal oxygens affect those distributions in the symmetrical carotenoids. The variation of only one side terminal group at the polyene chain (**1** and **3**) demonstrates similar strong influence on bond lengths and charge distribution.

AM1 calculations predict that protonation can produce several protonated forms of each carotenoid. The protonation sites with the lowest enthalpy ($\Delta\Delta H_0$ is within 5 kcal mol^{-1} above the minimum) are C7 < C11 < C5 < C9 (**1**); C7 < C5, C11 < C9, O (**2**); C9′ < O, C11′ < C15′ < C7 (**3**). This order is expected to be correct for the gas phase, but may be changed in the solution due to the differences in solvation energy of the carbocations. The contribution of solvation entropy also can be significant enough to change the resulting order of the pK_{BH} values of $(Car)_{trans}$, especially those which correspond to the carbocations with similar heats of formation. Unfortunately, the lack of data on solvation entropies does not allow one to calculate the pK_{BH} values. However, AM1 enthalpies allow one to predict the most probable protonation sites at the polyene chain and thus the composition of *cis*-isomers formed by protonation.

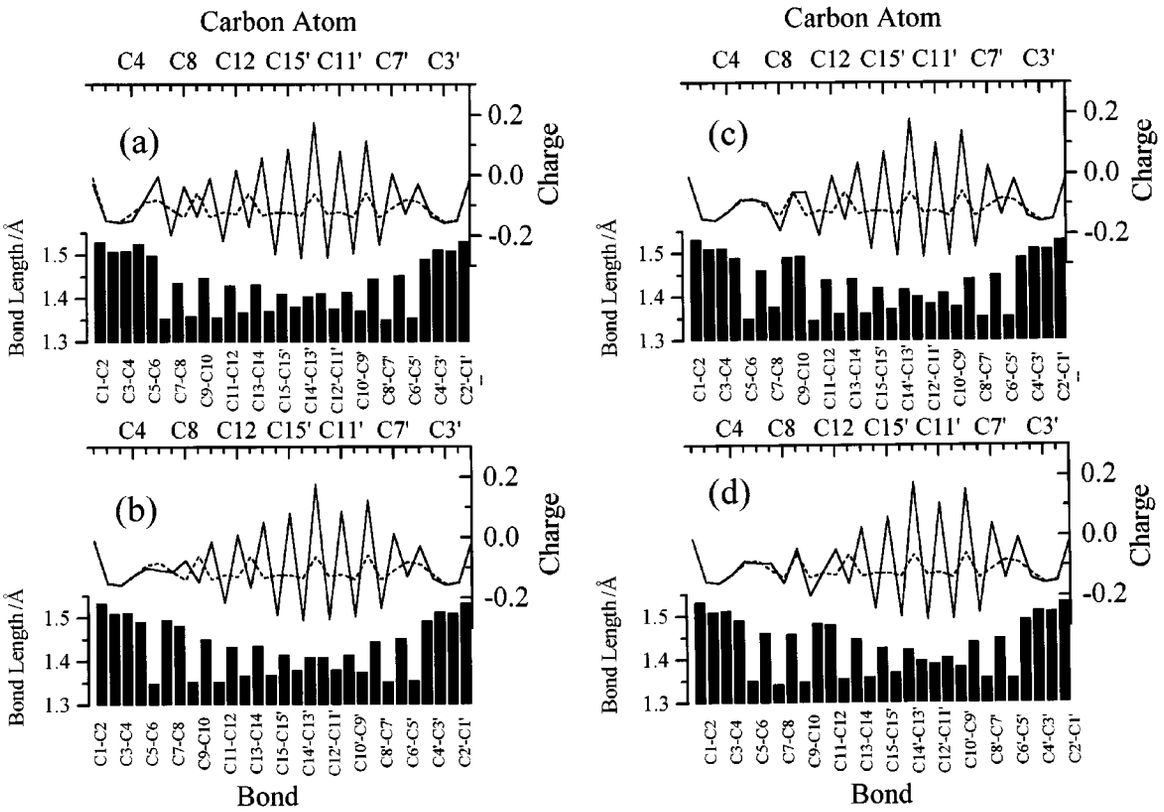

Fig. 1 a–d AM1 atomic charge and bond length (Å) for carbocations of **1**. (a) Protonation at C5, (b) at C7, (c) at C9, (d) at C15. Dotted line indicates the charge for neutral compound **1**.

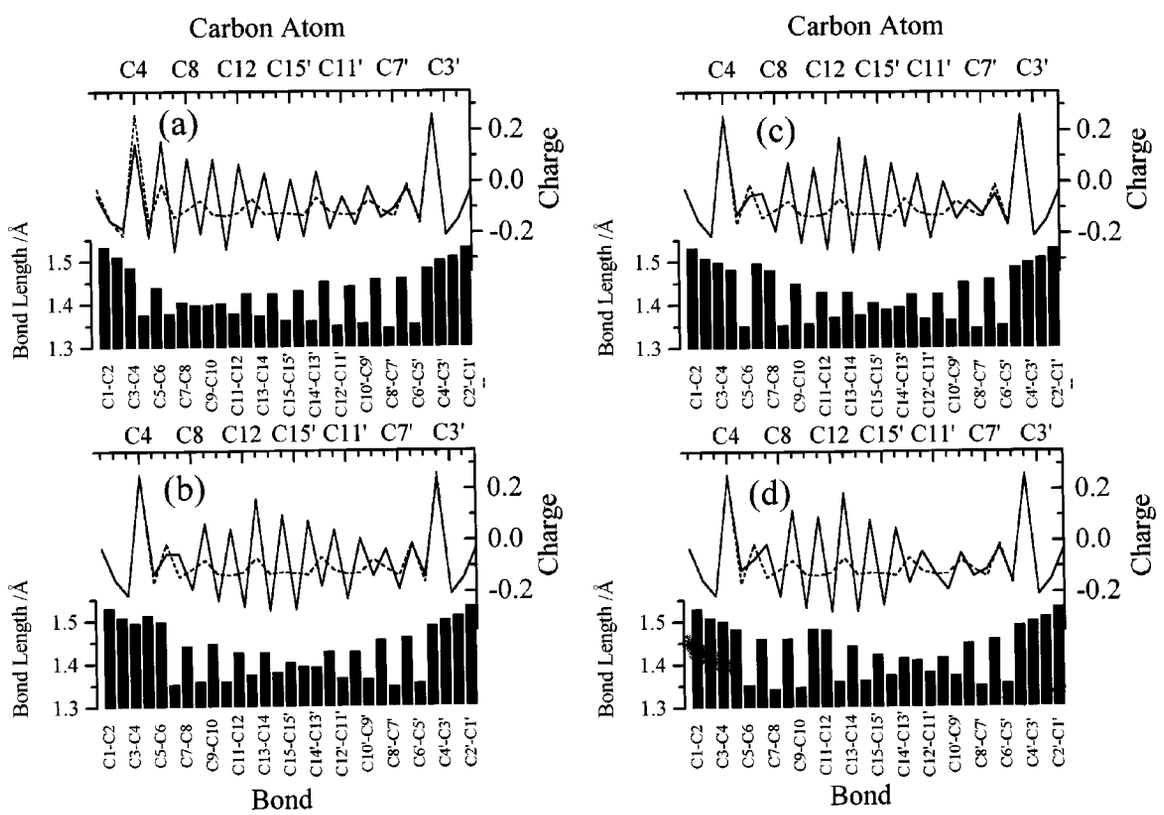

Fig. 2 a–d AM1 atomic charge and bond length (Å) for carbocations of **2**. (a) Protonation at oxygen, (b) at C5, (c) at C7, (d) at C11. Dotted line indicates the charge for neutral compound **2**.

The AM1 calculated dipole moments D of $CarH^+$ (PM3 calculations gave practically the same values of D) are much higher then that of the corresponding neutral molecules (0.024, 0.658 and 4.626 D for **1**, **2** and **3**, respectively) and differ considerably compared to each other. For example, in the case of **2,** D changes from 5.5 D (protonation at C7) to 32.1 D (at oxygen), of **3** from 6.3 D (at C9′) to 14.3 D (at oxygen). Because the solvation energy is expected to be greater for species with

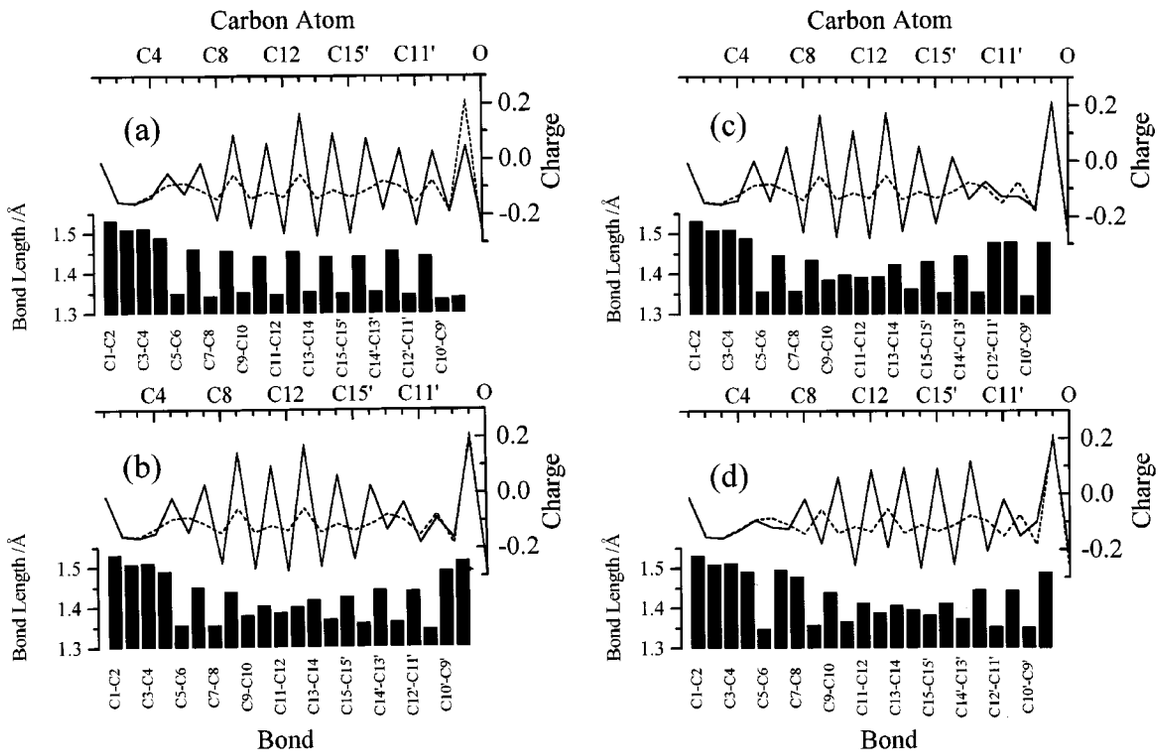

Fig. 3 a–d AM1 atomic charge and bond length (Å) for carbocations of **3**. (a) Protonation at oxygen, (b) at C9′, (c) at C11′, (d) at C7. Dotted line indicates the charge for neutral compound **3**.

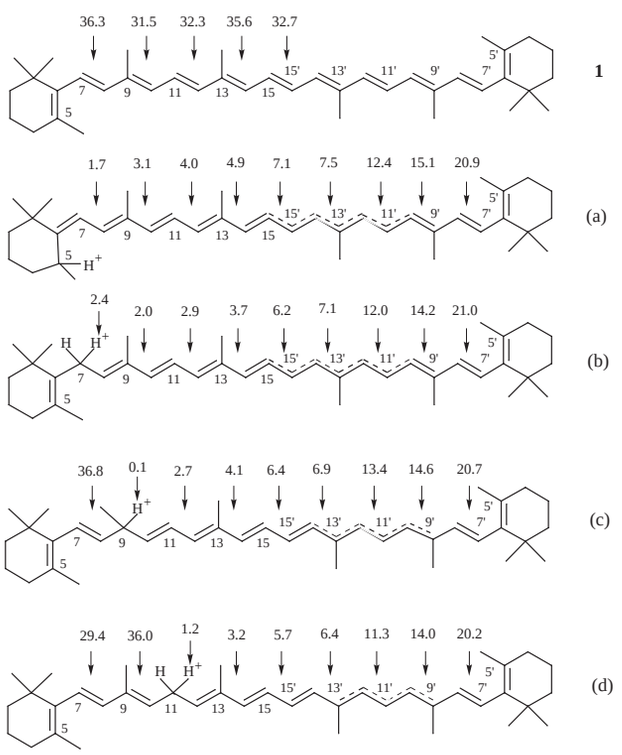

Fig. 4 The structures of the carbocations of **1** with the lowest heats of formation. Protonation at carbon atoms: (a) C5, (b) C7, (c) C9, (d) C11. The AM1 rotation barriers ΔH_{90} (kcal mol^{-1}) with respect to all-*trans* isomer are shown in italic.

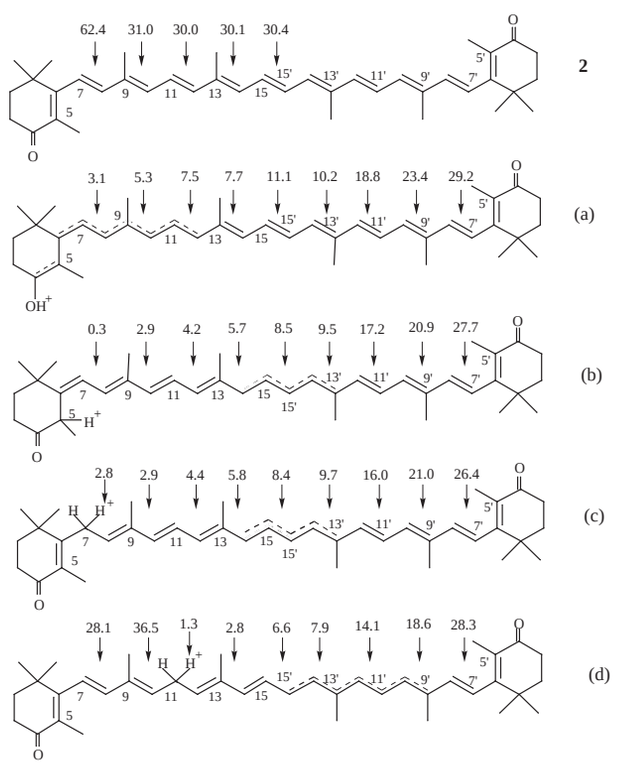

Fig. 5 The structures of the carbocations of **2** with the lowest heats of formation. (a) Protonation at oxygen; at carbon atoms: (b) C5, (c) C7, (d) C11.

greater dipole moments, protonation at oxygen in solution can become more favorable than at the C7 (**2**) or C9′ (**3**) chain carbons. As the relative permittivity of the solution increases, an increase occurs in the solvation energy of the ionic species, which may favor the formation of protonated forms with higher dipole moments. Thus the pK_{BH} values of the carotenoids and the composition of the protonated species are expected to be medium dependent.

cis-Isomerization

In order to predict which *cis*-isomers could be formed by the protonation of carotenoids, consideration must be given to the stabilities of the carbocations and to the activation enthalpy for *cis*-isomerization of carbocations.

The excess energy for 7-*cis* isomers (**1**–**3**) above that of the all-*trans* isomers was estimated as 35–48 kcal mol^{-1}.[28] In this study more extensive AM1 geometry optimization was per-

Table 2 The relative heats of formation ΔH_0 of *cis*-isomers with respect to the all-*trans*-isomer

	$\Delta\Delta H_0$/kcal mol^{-1}		
cis-Isomers	**1**	**2**	**3**
7	4.17	4.48	4.0
7,11	6.11	6.18	5.86
7,13	4.12	4.0	3.85
7,15	5.62	5.4	5.61
9	0.07	−0.05	0.17
9,11	2.38	2.0	2.33
9,13	0.07	−0.08	−0.06
9,15	1.42	1.39	1.28
9,9′	0.18	−0.2	0.96
9,13,9′	0.48	−0.03	0.84
9,13,13′,9′	−0.11	−0.26	0.75
11	2.38	2.14	2.1
11,13	3.51	2.80	2.78
11,15	3.72	3.58	3.45
11,13′	2.39	2.11	2.08
11,11	4.24	4.5	4.09
13	0.09	−0.01	0.11
13,15	1.43	1.32	1.33
13,13′	0.08	0.08	0.08
9,13,13′	0.91	−0.03	0.22
15	1.71	1.34	1.69
13′	—	—	0.08
13′,11′	—	—	2.32
13′,9′	—	—	0.96
11′	—	—	2.21
11′,9′	—	—	3.09
9′	—	—	0.09

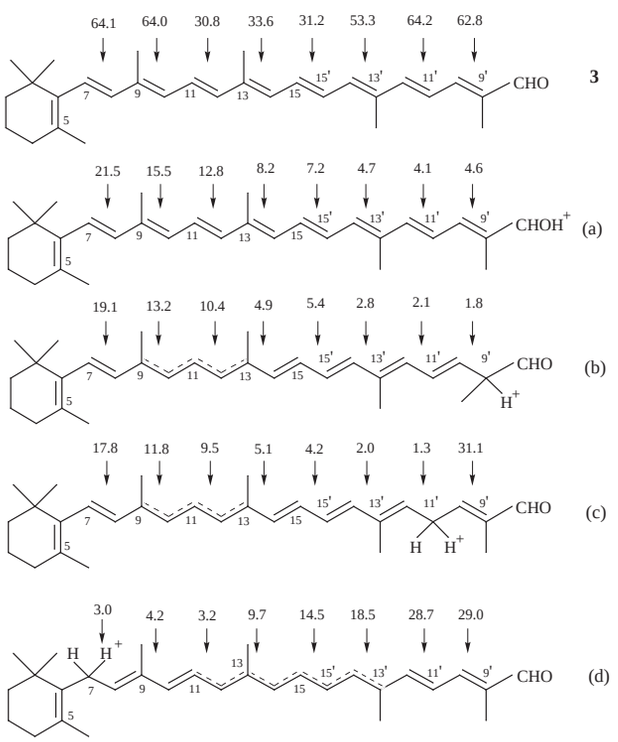

Fig. 6 The structures of the carbocations of **3** with the lowest heats of formation. (a) Protonation at oxygen; at carbon atoms: (b) C9′, (c) C11′, (d) C7.

formed. The calculated relative heats of formations $\Delta\Delta H_0$ of *cis*-isomers are presented in Table 2 and correspond well with molecular mechanics calculations.[23] It is seen that the heats of formations of all *cis*-isomers are similar and that the variation $\Delta\Delta H_0$ does not exceed 5 kcal mol^{-1}. The *cis*-isomers of **1** with the lowest $\Delta\Delta H_0 = -0.1$–0.2 kcal mol^{-1} are 9-*cis*, 13-*cis*, 9-*cis*-9′-*cis*, 13-*cis*-13′-*cis*, 9-*cis*-13-*cis*, 9-*cis*-13-*cis*-13′-*cis*-9′-*cis* (see

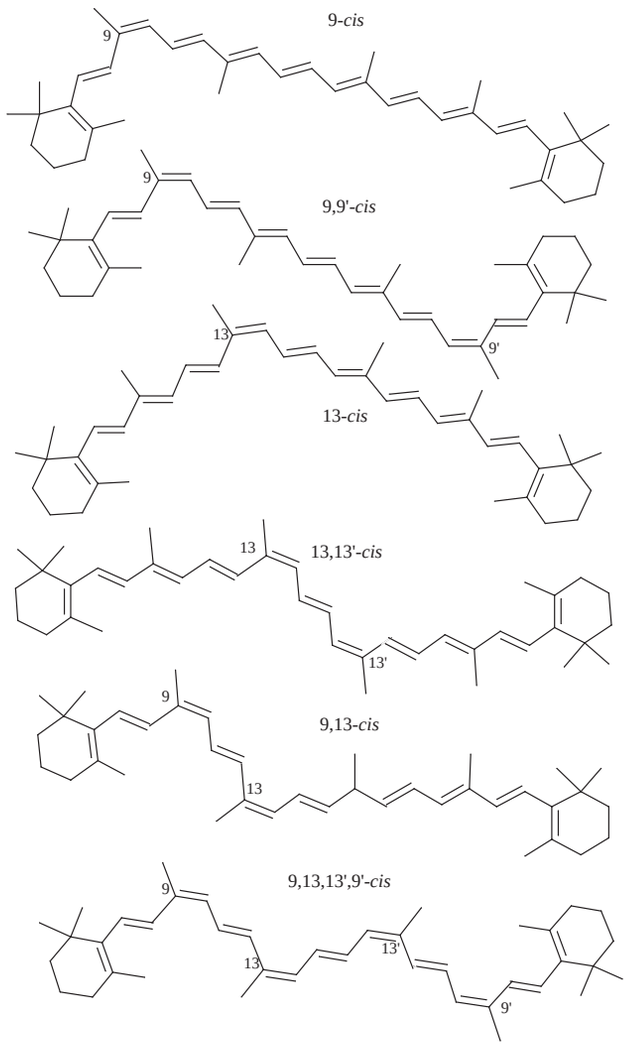

Fig. 7 Structures of the most favorable *cis*-isomers after protonation of **1**.

Fig. 7). For the symmetrical 9-*cis*-13-*cis*-13′-*cis*-9′-*cis* isomer of **2,** the $\Delta\Delta H_0$ was predicted to be 0.26 kcal mol^{-1} less then for the all-*trans* compound. For 7-*cis* and 11-*cis* isomers, severe distortion of the optimized structure with respect to the all-*trans* compound was obtained. This distortion was caused by steric interaction between the chain H-atoms and the methyl groups. Thus, we can conclude that with the exception of the 7-*cis* and 11-*cis* isomers, the relative enthalpy of the *cis*-isomers should not affect the acid-induced isomer distribution.

The activation enthalpy for *cis*-isomerization of carotenoid carbocations is unknown and can be estimated as the AM1 rotation barrier, ΔH_{90}, for the rotation about the corresponding bond. The ΔH_{90} values have been calculated as the excess enthalpy for the 90°-twist, when the corresponding dihedral angle has been frozen and the rest of the carbocation allowed to relax during AM1 geometry optimization. This approach was tested by comparison to the isomerization of neutral β-carotene (**1**) for which experimental activation enthalpy was known from thermal isomerization data.[24,27] The AM1 calculated ΔH_{90} values (see Fig. 4) 32.7 (*trans*→15-*cis*), 35.6 (*trans*→13-*cis*) and 32.3 kcal mol^{-1} (11-*cis*→*trans*) are very close to experimental ones: 28.9 ± 5,[24] 27.7 ± 1.5[24] and 23.4 ± 0.9 kcal mol^{-1},[27] respectively. Though ΔH_{90} values exceed the experimental activation enthalpies by 20–40% they can be used as a good approximation for the actual activation barrier. The calculated ΔH_{90} are shown in Figs. 4–6 and demonstrate that protonation of carotenoids generally decreases the rotation barrier for *cis*-isomerization. As expected, the ΔH_{90} values for "new

single bonds" are about 1–5 kcal mol^{-1}, which is typical for the rotation about a single bond, and for "new double bonds" are 20–36 kcal mol^{-1}, which is somewhat less then that for a double bond in the chain of neutral carotenoid.

cis-Isomerization is a thermo-activated process, and the composition of *cis*-isomers formed by protonation of carotenoids depends on temperature. Combining the data on rotational barriers for carbocations and stabilities of *cis*-isomers from Table 2, the most probable *cis*-isomers can be predicted for each temperature. Assuming "free rotation" about a bond with ΔH_{90} less than 5 kcal mol^{-1}, which is typical at room temperature (20–25 °C), the sites of *cis*-isomerization, shown in Table 3, can be predicted. The most probable *cis*-isomers produced by protonation of all-*trans* carotenoids at low temperature are shown in Table 4. In that case 7-*cis*, 11-*cis* and 9′-*cis* isomers and their di-isomers were excluded for thermodynamic reasons. Note, that those isomers were not observed among the products of low temperature (35–60 °C) thermolysis.[23] At higher temperature 7-*cis* and 11-*cis* isomers, as well as 15-*cis* and 13′-*cis* isomers, which have higher rotation barriers can be formed by protonation of all-*trans* carotenoids. *cis*-Isomers also can be protonated to produce di- and higher multi-*cis*-isomers even at low temperature, *i.e.* 13-*cis*-13′-*cis*, 9-*cis*-13′-*cis*, 9-*cis*-13′-*cis*, 9-*cis*-9′-*cis*, 9-*cis*-13-*cis*-13′-*cis*, 9-*cis*-13-*cis*-13′-*cis*-9′-*cis*.

AM1 predicted *cis*-isomers of carotenoids could be compared with experimental HPLC data for the products identified in 3 mM solution of **2** and **3**[28] in CH_2Cl_2 with 0.1–0.2 mM HCl[28] (see Table 4). The composition of the *cis*-isomer mixture after protonation corresponds well to the theoretical prediction. The presence of the di-isomer, 13′-*cis*-13′-*cis*, among the products of **2** can result from the second protonation of its 13-*cis* isomer. A distinction between that predicted and the data of ref. 28 for compound **3** could be a result of assigning the 13′-*cis* or 11′-*cis* retention peaks to the 13-*cis* isomer. A NMR analysis of the products is necessary to elucidate this problem, but has not been carried out.

TLC analysis of the protonated products of **1**–**3** in benzene after re-isolation from alkaline water, resulted in the return of the orange color for **2** and **3**. For **3** only one product (>90%) identical to the starting all-*trans* compound was observed. However, for **2,** two orange color products in addition to the all-*trans*, which was dominant, were observed. The preferred protonation site for **3** is the oxygen, which forms a few *cis*-isomers after de-protonation. For **2** there are two places for protonation resulting in two isomers. Preliminary NMR (^1H, 360 MHz,) data obtained for **3** in $CDCl_3$ in the presence of 1–10 mM CF_3COOD (at 20–22 °C) showed the presence of an olefinic region with broad peaks, which is typical for carbocationic species. A large shift of the H10′ proton strongly supports the protonation at oxygen. For **2** the NMR spectra after addition of the same amount of acid were different from that observed for **3**. The olefinic peaks completely disappeared and the aliphatic peak positions for the protons in the chain methyl groups also changed. Thus the carbocations of **2** and especially of **1** undergo fast decomposition at room temperature. The possible reason for decomposition observed by NMR and TLC experiments could be bimolecular reactions of $CarH^+$ due to the relatively high concentration of carotenoids (1–5 mM). In an attempt to avoid complications due to bimolecular reactions, we thereafter studied the $CarH^+$ properties by optical spectroscopy, which enable us to work at very low carotenoid concentrations.

Table 3 The positions for *cis*-isomerization predicted from AM1 calculations of all-*trans* carotenoids. Number of stars (*) qualitatively corresponds to the most preferable protonation sites

Protonation site	Positions for *cis*-isomerization		
	1	**2**	**3**
Oxygen		**7	***13′,11′,9′
C5	**7,9,11,13	***7,9,11	*
C7	***7,9,11,13	***7,9,11	**7,9,11
C9	**9,11,13	**9,11,13	—
C11	***11,13	***11,13	—
C15′	—	—	**13,15
C11′	—	—	***13,15,13′,11′
C9′	—	—	***13,15,13′,11′,9′

Optical spectra

Optical spectra of protonated adducts of **1**–**3** were measured in benzene, CH_2Cl_2 and acetonitrile solutions in the presence of different amounts of trifluoroacetic acid (TFA) (see Figs. 8–10). The carotenoid concentration was 0.2–0.5 μM, so that the

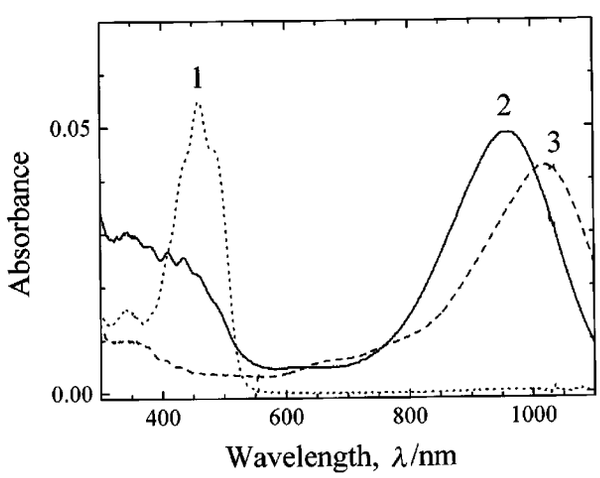

Fig. 8 Optical spectra of **1** solution in benzene (0.44 μM) and in CH_2Cl_2 (0.275 μM) before and 10–15 s after mixing with TFA. (1) Benzene, no acid; (2) benzene, 0.29 v% of TFA; (3) 0.275 μM in CH_2Cl_2, 0.22 v% of TFA.

Table 4 The most probable *cis*-isomers at ambient temperature (20–25 °C) produced by acid induced isomerisation

	1	**2**	**3**
AM1 predicted *cis*-isomers produced from all-*trans* carotenoids	9-*cis*, 13-*cis* 9-*cis*-13-*cis*	9-*cis*, 13-*cis* 9-*cis*-13-*cis*	13′-*cis*, 11′-*cis* 13′-*cis*-11′-*cis*
Experiment (HPLC) with 0.1–0.2 mM HCl in CH_2Cl_2[a]	—	all-*trans* (62.1%) 9-*cis* (14.8%) 13-*cis* (14%) 13′-*cis*-13′-*cis* (2.7%)	all-*trans* (68.8%) 13-*cis* (15.6%) 13′-*cis*-11′-*cis* (12%)
Re-isolation experiment (TLC) with 10 mM TFAA in CH_2Cl_2	no all-*trans*; not characterized products	all-*trans* (80–90%) 2 main isomers, not characterized	all-*trans* (>90%)

[a] Ref. 28.

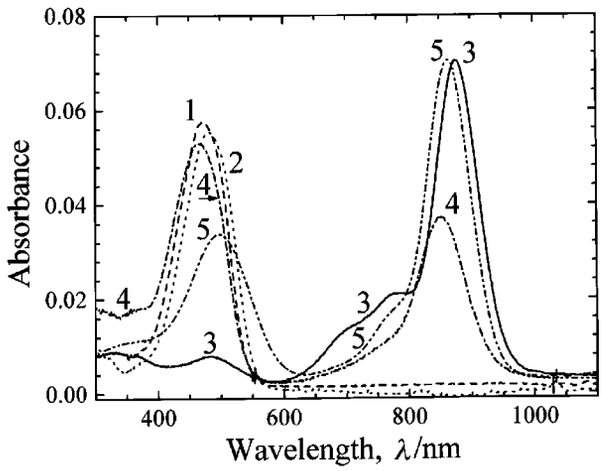

Fig. 9 Optical spectra of 0.44 μM solution of **2** in different solvents. (1) Acetonitrile, no acid; (2) CH_2Cl_2, no acid; (3) CH_2Cl_2, 0.58 v% of TFA; (4) acetonitrile, 0.72 v% of TFA; (5) benzene, 6.25 v% of TFA.

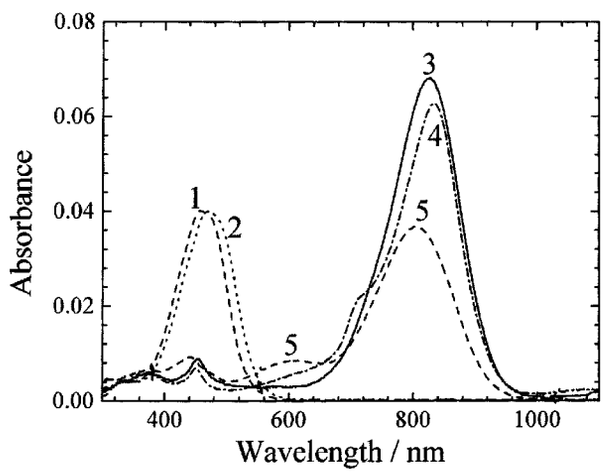

Fig. 10 Optical spectra of 0.36 μM solution of **3** in different solvents. (1) Acetonitrile, no acid; (2) CH_2Cl_2, no acid; (3) benzene, 6.25 v% of TFA; (4) CH_2Cl_2, 6.25 v% of TFA; (5) acetonitrile, 6.25 v% of TFA.

acid was always in great excess. Two mixing orders were tried and both gave the same results, *i.e.* concentrated carotenoid solution was injected into the acid solution, or pure acid was injected into carotenoid solution. The lifetime of carbocations was strongly dependent on the solvent and decreased with increasing acid concentration. In CH_2Cl_2, protonated adducts were the most stable and their half-life times, $t_{1/2}$, at low acid concentrations (<1 v%) were in the range of 1–3 hours. In benzene and acetonitrile adducts were much less stable having $t_{1/2}$ about 30–50 s (**1, 2**) and 300–700 s (**3**). At the limits of low carotenoid and acid concentration, the optical spectra are due to the carotenoid carbocations $CarH^+$. The complicated chemistry of carotenoid carbocations deserves to be examined separately. In this paper we restrict our consideration to the influence of solvent on the optical spectrum of $CarH^+$ after initial protonation.

The optical spectra of **1** in benzene recorded just after mixing with the TFA (Fig. 8) show that the absorption of the neutral carotenoid near 460 nm completely disappeared after mixing. At low acid concentration (<1 v%) there is a new single peak at λ_{max} = 962 nm. The peak intensity decreases with time and λ_{max} shifts to 923 nm. Such behavior can be attributed to carbocation *cis*-isomerization by analogy to the blue shift that occurs upon *trans* to *cis*-isomerization of carotenoids,[28,36,37] although the shift is somewhat larger than for neutral molecules. The optical spectrum of **1** in CH_2Cl_2 (Fig. 8) is similar to that in benzene, but the maximum is red shifted (λ_{max} = 1022 nm).

Table 5 Optical characterstics (λ_{max}/nm, 10^{-5} ε/M^{-1} cm^{-1}) of carbocations in different solvents

	1		**2**		**3**	
Solvent	λ_{max}	10^{-5} ε	λ_{max}	10^{-5} ε	λ_{max}	10^{-5} ε
Benzene[a]	962		863	2.92	826	1.87
CH_2Cl_2[a]	1022	1.86	881	2.91	844	1.72
Acetonitrile[a]	—	—	853		803	1.01

[a] In presence of TFA (0.29 v%). *T* 21 °C.

The initial optical spectrum of **2** in CH_2Cl_2 (Fig. 9) shows a narrower peak (λ_{max} = 878 nm) than of **1**, but also displays shoulders at 710 and 785 nm. At higher acid concentration only a peak at 785 nm was observed, and a shoulder at 710 nm developed during the decay. Thus, the latter can be attributed to the decay product of $CarH^+$. In benzene and acetonitrile in the presence of TFA both red (863 and 853 nm, respectively) and blue peaks (493 nm and 455 nm) are observed although in CH_2Cl_2 the blue peak is almost absent. In our opinion, the blue peaks cannot be attributed to residual starting carotenoid, because at such acid concentrations (3–6 v%) the absorption of the starting compound was not observed for **2** in CH_2Cl_2 or for **1** in all solvents. This conclusion is also supported by the fact that the absorbance of protonated adduct of **2** at 455 nm in acetonitrile is the same as that of the starting neutral compound, which should be consumed in the protonation reaction. The larger extinction coefficients of $CarH^+$ relative to the neutral compound could explain this effect.

The optical spectra of **3** in the presence of acid generally consist of a single relatively narrow peak with λ_{max} about 800–840 nm in all solvents. The position of this peak is nearly unchanged with increasing TFA concentration from 0.2 to 6.25 v%.

The extinction coefficients, ε, of $CarH^+$ were estimated from the time dependence of λ_{max} by extrapolation to zero time, and are presented in Table 5. Extinction coefficients of neutral carotenoids were used as references; **1**: 1.36×10^5 M^{-1} cm^{-1} (acetonitrile), 1.24×10^5 M^{-1} cm^{-1} (benzene), 1.27×10^5 M^{-1} cm^{-1} (CH_2Cl_2); **2**: 1.18×10^5 M^{-1} cm^{-1} (benzene), 1.26×10^5 M^{-1} cm^{-1} (CH_2Cl_2); **3**: 1.1×10^5 M^{-1} cm^{-1} (all solvents).

The optical spectra demonstrate that the position of the absorption maximum (λ_{max}) of $CarH^+$ is very close to the carotenoid radical cation $Car^{\bullet+}$, λ_{max} = 800–1000 nm.[28,38] However, the radical cation can be excluded from consideration, because carotenoid solutions at low concentrations (<1 mM) did not have an EPR signal at any acid concentration (to increase the EPR sensitivity and to avoid $CarH^+$ degradation, carotenoid solutions were frozen immediately at 77 K, 1–2 s after mixing with acid). Note, that EPR signals were observed for more concentrated carotenoid solutions (>5 mM), as well as when solid pieces of carotenoids were added into acidic solution. The similarity of the optical spectra of $CarH^+$ and $Car^{\bullet+}$ indicate that one should be cautious in using absorptions near 800–1000 nm as a finger-print of carotenoid radical cations.

From Figs. 8–10 we can conclude that optical spectra of $CarH^+$ depend only slightly on the nature of the solvent. Single optical peaks for **1** and **3** are an indication that a single carbocation was formed. In the case of **2**, two peaks also can represent the same carbocation. The protonation of **1** occurs at the polyene chain, but at oxygen for **2** and **3**, as has been discussed before in the AM1 calculation section and demonstrated for **3** by NMR techniques. Thus the solvation energy of $CarH^+$ even in such low polarity solvent as benzene is sufficient to make the protonation at oxygen more favorable than at the chain for **3,** and probably for **2**. In order to confirm that the optical spectrum of $CarH^+$ can have several optical peaks, we carried out INDO/S calculations for **1**, **2** and **3**.

Table 6 INDO/S wavelengths λ_{max} and oscillator strengths (>0.1) of the two most intense electronic transitions in the region > 270 nm

	1		**2**		**3**	
Protonation position	λ_{max}/nm	Oscillator strength	λ_{max}/nm	Oscillator strength	λ_{max}/nm	Oscillator strength
Oxygen	—	—	702	3.39	645	3.37
			358	0.51	272	0.30
C5	700	3.43	661	3.54	636	3.49
					323	0.38
C7	641	3.25	613	3.32	578	3.28
			271	0.39		
C9	596	2.99	581	3.17	533	2.85
			260	0.52	460	0.24
C11	561	2.75	542	2.90	568	0.52
			269	0.85	461	2.34
C15′	—	—	—	—	497	2.07
					283	1.18
C13′	—	—	—	—	522	2.50
					337	0.31
C11′	—	—	—	—	558	2.76
					368	0.23
C9′	—	—	—	—	597	3.00
Starting molecule	396	3.70	404	3.75	435	2.59
			290	0.41	336	0.15
Radical			635	3.49	658	1.19
Cation			289	0.48	621	1.99
Dication	559	4.11	563	4.01	539	3.76
			345	0.42	394	0.23

INDO/S optical transitions

AM1 optimized carbocation geometry was used as input for single point INDO/S calculations of the carbocation optical spectra. The wavelength λ_{max} and the oscillator strength of the two most intense electronic transitions are shown in Table 6. For protonation near the end of the chain, the optical transition consists of only one intense peak. For protonation at the center of the chain, a second peak becomes comparable in intensity to the first one whose intensity decreases. For $CarH^+$ with terminal protonation sites, the optical transitions occur at longer wavelengths than that for $CarH^+$ with center protonation sites. Thus INDO/S calculations demonstrate that $CarH^+$ can have two intense optical transitions. For example, the carbocation of **2** protonated at oxygen exhibits transitions at 358 and 702 nm.

Calculated wavelengths of the optical transitions of $CarH^+$ are 200–300 nm less than the experimental λ_{max} of the protonated adducts, however, in much the same way INDO/S method gave lower values for optical transitions of $Car^{\bullet+}$ compared to experimental data (*e.g.* 635 nm for $Car^{\bullet+}$ of **1**, instead of 1020 nm).[39] The possible reason of such over-estimation of the electronic energy of the carotenoid cations is that a number of excited states used in our INDO/S calculations (*i.e.* 100–120) is not enough to correctly predict the optical spectrum of the long polyene chains. Nevertheless, the INDO/S technique does predict the general trends for the optical spectra of $CarH^+$, which are in line with experimental observations.

Conclusion

The mechanism of the acid-induced carotenoid *trans–cis* isomerization includes the formation of the intermediate carbocation, $CarH^+$, in which the barrier for rotation about the corresponding bond is sufficiently less (down to 0–5 kcal mol^{-1}) than for the neutral carotenoid. AM1 calculated enthalpies of formation of $CarH^+$ indicate that multiple protonation sites for carotenoid polyene chain molecules are possible, which do not correlate with the electron density in the starting molecule. The terminal substituents affect both the possible protonation sites and the yield of *cis*-isomers.

Optical spectra of $CarH^+$ solutions exhibit new peaks in the range of 700–1020 nm; they are very close to the optical spectra of the corresponding radical cations, $Car^{\bullet+}$. Peak wavelength and extinction coefficients of $CarH^+$ depend on solvent.

The AM1 predicted dipole moments D of $CarH^+$ differ considerably and can reach very high values, *i.e.* for **2,** $D = 5.5$ D (protonation at C7) and 32.1 D (at oxygen). Thus, acid-carotenoid solutions (which are stable for hours at ambient temperature) may be very promising for nonlinear optic applications.

Acknowledgements

This work was supported by the US Department of Energy, Office of Basic Energy Sciences, Division of Chemical Sciences, Grant DE-FG02-86ER13465. We thank Dr Elli Hand for helpful discussions.

References

1 Y. Koyama, *J. Photochem. Photobiol. B*: *Biol.*, 1991, **9**, 265.
2 H. A. Frank, C. A. Violette, J. K. Trautman, A. P. Shreve, T. G. Owens and A. C. Albrecht, *Pure Appl. Chem.*, 1991, **63**, 109.
3 M. Mimuro and T. Katoh, *Pure Appl. Chem.*, 1991, **63**, 123.
4 R. V. Bensasson, E. J. Land and T. G. Truscott, *Excited States and Free Radicals in Biology and Medicine*, Oxford University Press, Oxford, 1993.
5 G. E. Bialek-Bylka, T. Hiyama, K. Yumoto and Y. Koyama, *Photosynth. Res.*, 1996, **49**, 245.
6 G. E. Bialek-Bylka, T. Tomo, K. Satoh and Y. Koyama, *FEBS Lett.*, 1995, **363**, 137.
7 J. Deisenhofer and H. Michel, *Science*, 1989, **245**, 1463.
8 M. Kuki, Y. Koyama and H. Nagae, *J. Phys. Chem.*, 1991, **95**, 7171.
9 A. Bendich and J. A. Olson, *FASEB J.*, 1989, **3**, 1927.
10 A Farmilo and F. Wilklinson, *Photochem. Photobiol.*, 1973, **18**, 447.
11 F. Wilklinson and W.-T. Ho, *Spectrosc. Lett.*, 1978, **11**, 455.
12 M. A. J. Rodgers and A. L. Betes, *Photochem. Photobiol.*, 1980, **31**, 533.
13 O. T. Kasaikina, Z. S. Kartasheva and A. B. Gagarina, *Izv. Akad. Nauk SSSR*, *Ser. Khim.*, 1981, 536.
14 G. W. Burton and K. U. Ingold, *Acc. Chem. Res.*, 1986, **19**, 194.
15 K. U. Ingold, W. W. Bowry, R. Stoker and C. Walling, *Procl. Natl. Acad. Sci. USA*, 1993, **90**, 45.
16 W. W. Bowry and R. Stoker, *J. Am. Chem. Soc.*, 1993, **115**, 6029.
17 N. I. Krinsky, *Free Radical Biol. Med.*, 1989, **7**, 617.
18 R. Peto, Doll, J. D. Buckley and M. B. Sporn, *Nature*, 1981, **290**, 201.
19 R. G. Ziegler, *Am. J. Clin. Nutr.*, 1991, **53**, 251S.

20 W. F. Malone, *Am. J. Clin. Nutr.*, 1991, **53**, 305S.
21 M. M. Mathews-Roth, *Pure Appl. Chem.*, 1991, **63**, 147.
22 R. S. Becker, *Photochem. Photobiol.*, 1988, **48**, 369.
23 W. v. E. Doering, C. Sotiriou-Leventis and W. R. Roth, *J. Am. Chem. Soc.*, 1995, **117**, 2747.
24 W. v. E. Doering and T. Kitagawa, *J. Am. Chem. Soc.*, 1991, **113**, 4288.
25 K. Tsukida, K. Saiki and M. Sugiura, *J. Nutr. Sci. Vitaminol.*, 1981, **27**, 551.
26 K. Tsukida and K. Saiki, *J. Nutr. Sci. Vitaminol.*, 1983, **29**, 111.
27 Y. Hu, H. Hashimoto, G. Moine, U. Hengartner and Y. Koyama, *J. Chem. Soc.*, *Perkin Trans. 2*, 1997, 2699.
28 A. S. Jeevarajan, C. C. Wei and L. D. Kispert, *J. Chem. Soc.*, *Perkin Trans. 2*, 1994, 861.
29 M. Zardkoohi, J. F. Haw and J. H. Lunsford, *J. Am. Chem. Soc.*, 1987, **109**, 5278.
30 *Carbonium Ions*, Vol. 2, eds. G. A. Olah and P. v. R. Schleyer, Wiley-Interscience, New York, 1970, p. 963.
31 *Stable Carbocation Chemistry*, eds. G. K. S. Prakash and P. v. R. Schleyer, Wiley-Interscience, New York, 1997, p. 587.
32 R. Kuhn and C. Grundmann, *Chem. Ber.*, 1938, **71B**, 442.
33 A. J. Wassermann, *J. Chem. Soc.*, 1954, 4329.
34 A. J. Wassermann, *J. Chem. Soc.*, 1959, 986.
35 T. S. Sorensen, *J. Am. Chem. Soc.*, 1965, **87**, 5075.
36 Y. Koyama, T. Takii, K. Saiki and M. Tsukida, *Photochem. Photobiophys.*, 1983, **5**, 139.
37 *Carotenoids. Volume 1B: Spectroscopy*, eds. G. Britton, S. Liaaen-Jensen and H. Pfander, Birkhäuser Verlag, Basel-Boston-Berlin, 1995, pp. 13–62.
38 M. Khaled, A. Hadjipetrou and L. D. Kispert, *J. Phys. Chem.*, 1990, **94**, 5164.
39 J. A. Jeevarajan, C. C. Wei, A. S. Jeevarajan and L. D. Kispert, *J. Phys. Chem.*, 1996, **100**, 5637.

Paper 8/00551F